Enhanced Mechanical Properties through Reversion in Metastable Austenitic Stainless Steels

M.C. SOMANI, P. JUNTUNEN, L.P. KARJALAINEN, R.D.K. MISRA, and A. KYRÖLÄINEN

A novel processing route of cold rolling and reversion annealing for enhanced mechanical properties has been investigated in metastable 17Cr-7Ni-type austenitic stainless steels, *i.e.*, commercial grades AISI 301LN and AISI 301, and in some experimental heats. The investigation was essentially aimed at studying the possibility of processing nano/submicron-grained structure in these steels and to rationalize the possible effects of alloying elements on the reversion mechanisms. The steels were cold rolled to various reductions between 45 and 78 pct to induce the formation of martensite, and subsequently annealed between 600 °C to 1000 °C for short annealing times (mostly 1 to 100 seconds). Microstructure examinations of the reversion-annealed 301LN steel revealed that an ultrafine-grained austenitic structure was formed by the diffusional transformation mechanism within a short holding time above 700 °C, even after the lowest cold-rolling reduction. In contrast, in 301 steel and experimental heats, the shear type of transformation occurred at temperatures above 650 °C, but fine austenite grains were only formed by recrystallization at higher temperatures or longer holding times, *e.g.*, at 900 °C/100 s. An attempt has been made to determine the reversion mechanisms in various steels by modifying the criteria governing the Gibbs free energy change during the martensite-austenite reversion in Cr-Ni alloys. The room temperature (RT)-tensile property evaluation showed that excellent combinations of yield or tensile strength and elongation are possible to achieve, depending mainly on annealing conditions both in the 301LN and 301 steels, but the experimental heats were too unstable for high ductility. Ultrafine grain size of austenite contributed to this in 301LN and shear-transformed high-dislocated austenite in 301. Upon reversion annealing, the reversion mechanism did not affect the texture. The texture of the reverted fine-grained austenite is very strong compared to the typical texture of commercially cold-rolled and annealed 301LN steel.

DOI: 10.1007/s11661-008-9723-y

I. INTRODUCTION

THE demerit of annealed austenitic stainless steels is that their yield strength ($R_{p0.2}$) is quite low, *e.g.*, 230 to 260 MPa for AISI 304 type, and 350 to 380 MPa for AISI 301LN. Tensile strength (R_m) is in the range of 600 to 800 MPa and total elongation from 45 to 60 pct. An interest in improving the mechanical properties of common austenitic stainless steels so that they could be better used, *e.g.*, in structural applications and automotive safety components, has led to the development of new processing routes.[1,2] As is well known, nitrogen alloying is quite beneficial in increasing the strength by the solid-solution strengthening.[3] However, there is a low limit for nitrogen solubility in conventional grades and problems with hot ductility may also appear with increased nitrogen content. Cold rolling is a technique applied industrially to increase the strength. The yield strength of austenitic stainless steels, and particularly that of metastable alloys, can be drastically improved by cold deformation that generates strain-induced martensite in addition to ordinary strain hardening of high-alloyed austenite. However, ductility is consequently decreased. The strength levels of commercial temper-rolled grades are classified in the design manual for structural stainless steel.[4] Typical reported values for C850 (1/4 Hard) grade are $R_{p0.2} \approx 650$ MPa, $R_m \approx 970$ MPa, and the total elongation $A_{80} \approx 30$ pct.[5] Partial annealing of cold-rolled structure has been found to enhance combination of strength and ductility for AISI 304, $R_{p0.2} \approx 450$ MPa and 40 pct elongation.[6] A special process of thermomechanical treatment consisting of a double cold-deformation annealing cycle for a 10Cr-5Ni-8Mn steel has resulted in a combination of $R_{p0.2} \approx 780$ MPa, $R_m \approx 1100$ MPa, and 30 pct elongation, based on nanosized grain structure.[7]

In this context, a novel processing route of controlled reversion annealing of the heavily cold-deformed

M.C. SOMANI, Senior Researcher, P. JUNTUNEN, Researcher, and L.P. KARJALAINEN, Professor, are with the Materials Engineering Laboratory, Department of Mechanical Engineering, University of Oulu, 90014 Oulu, Finland. R.D.K. MISRA, Professor of Materials Science and Engineering and Director, is with Center for Structural and Functional Materials, University of Louisiana at Lafayette, LA 70504-4130. Contact e-mail: dmisra@louisiana.edu A. KYRÖLÄINEN, General Manager, is with the Raahe Region Technology Center Ltd., 92100 Raahe, Finland.

Manuscript submitted April 24, 2008.
Article published online January 13, 2009

martensite in metastable Cr-Ni austenitic stainless steels has been employed resulting in highly refined austenite grain size.[8,9] In the first stage, the deformation of austenite in the vicinity of room temperature (RT) leads to strain-induced shear transformation of austenite to martensite, and then upon annealing this heavily deformed martensite transforms back to fine-grained austenite either through a martensitic shear or diffusional reversion mechanism.[8,9] An optimized annealing schedule leads to the formation of an ultrafine (nano- or submicron) grained structure. Submicron grain sizes have been obtained in laboratory heats of 18Cr-9Ni and 16Cr-10Ni types and in commercial AISI 304 and AISI 304L grades.[8–12] Fine grain size not only results in a significantly higher strength,[8,13,14] but also renders the material ductile and amenable for subsequent forming operation, *cf*. Reference 15. The reverted austenite may partially or fully transform back to the martensite phase in the course of forming or bending, thus further enhancing the final strength.

The present investigation forms a part of the research program concerning use of high-velocity forming methods to fabricate components of locally softened cold-rolled sheets. As the initial task, the present study concerns mainly the formation of submicron-grained, high strength austenitic stainless steels with enhanced yield and tensile strengths and reasonable ductility. Preliminary results concerning the microstructures and properties obtained on the reversion-annealed austenitic 17Cr-7Ni stainless steel grades AISI 301 and AISI 301LN have been presented elsewhere.[16–20] It was shown[16,17,20] that with a mixed phase structure combining martensite and mainly ultrafine austenite (and some deformed untransformed prior austenite), a high yield strength of about 1000 MPa with the elongation ~35 pct was achievable through controlled reversion annealing. On the other hand, a completely reverted ultrafine structure gave yield strength levels of the order of 600 MPa with a total elongation of ~50 pct.

Reversion process and formation of ultrafine austenite grain size resulting in enhanced strength-ductility combination have been briefly reported previously.[16,17,20] However, this article presents a detailed account of the effects of cold-rolling reduction and annealing parameters on the reversion characteristics of commercial AISI 301LN and AISI 301 steel grades, in comparison with those of some special Cr-Ni steels. A summary of the reversion mechanisms, microstructures and mechanical properties, strain hardening characteristics, and crystallographic texture development are presented.

II. MATERIALS AND EXPERIMENTAL DETAILS

The selected commercial steels AISI 301LN (EN1.4318) and AISI 301 (EN1.4310) were supplied by Outokumpu Oyj, Tornio Works (Tornio, Finland). The initial materials were annealed strips 1.5 mm in thickness taken from the production. These strips were cold rolled to the total reductions between 45 and 77 pct in a laboratory rolling mill using different pass reductions. After each rolling pass, the martensite fraction was determined by a Ferritescope MP30 instrument (Fischer Instrumentation (G.B.) Ltd., Hampshire, England), the reading multiplied by 1.7, a factor determined elsewhere.[21] The compositions of the two steels are given in Table I. In addition, three experimental Mn and Si free Cr-Ni heats, coded as 16/10, 17/7N, and 17/7C, were also vacuum-cast and rolled to compare the effects of chemical composition on microstructures, properties, and reversion mechanisms. The compositions of these experimental steels are also included in Table I. The composition of 16/10 is equal to that of the steel used in several prior investigations,[8,9,11–13] thus forming a reference material. An austenite stability index, M_{d30} temperature, as proposed by Nohara *et al*.,[22] has also been given in Table I.

Samples were cut from the cold-rolled strips in various stages of rolling, ranging from 45 to 77 pct reduction for reversion-annealing studies. The reversion-annealing experiments were carried out on a Gleeble 1500 simulator (Dynamic Systems Inc., Poestenkill, NY) on strips of 120 × 10 mm (thickness about 0.34 to 0.86 mm). The heating rate to the holding temperature was 200 °C/s. The annealing temperatures were in the range 500 °C to 1000 °C and the holding times selected were primarily in the range 0 and 10 seconds (100 and 1000 seconds in exclusive cases). The uniform temperature zone in the middle of the specimens was estimated to be about 20 mm in length. Following the annealing, all samples were cooled in air blow with cooling rates at least 200 °C/s down to about 400 °C.

The microstructures were examined with an optical microscope (OM), a transmission electron microscope (TEM), and a scanning electron microscope (SEM) equipped with an electron backscattered diffraction (EBSD) detector. While optical microscopy gave a qualitative image of the ultrafine microstructures, an assessment and comparison of grain size were carried out by SEM-EBSD and TEM techniques. The phase fractions were mainly determined by X-ray diffraction (XRD) using the Mo K_α radiation and the intensity

Table I. Chemical Compositions of the Tested Stainless Steels (Mass Percent)

Steel	C	Si	Mn	Cr	Ni	Mo	N	M_{d30}*(°C)
301LN	0.017	0.52	1.29	17.3	6.5	0.15	0.1500	26.6
301	0.100	1.06	1.18	16.7	6.3	0.65	0.0740	20.8
16/10	0.008	0.01	0.04	15.9	10.0	0.0	0.0045	36.7
17/7N	0.025	0.17	0.04	17.2	7.1	0.0	0.1150	42.6
17/7C	0.095	0.16	0.04	17.0	7.0	0.0	0.0205	59.7

*Reference 22.

peaks $(220)_\gamma$, $(311)_\gamma$, and $(211)_{\alpha'}$; verified in some cases by magnetic measurements using a Ferritescope MP30 instrument and a SQUID device (University of Texas, Austin, TX[18,19]). Even though XRD is considered to be a reliable technique, the precise determination of the martensite/austenite phase fractions remains a difficult task owing to problems such as texturing as discussed by Talonen *et al.*[21] However, Miller's method was considered appropriate in computing the phase fractions to minimize the effects of texture.[23]

Mechanical properties of the cold-rolled and reversion-annealed specimens were essentially determined by tensile testing in a 1000-kN Zwick machine at Outokumpu Research Centre, Tornio, Finland by machining a profile of 25 × 25 mm (or 20 × 20 mm) with a 20-mm gage length. This nonstandard geometry had to be used due to the narrow uniform annealed zone in Gleeble experiments. In addition, martensite formed at different stages of tensile testing was estimated for select specimens as using a Ferritescope instrument.[21] These results were further corroborated by Vickers hardness measurements.

The crystallographic textures were studied in the subsurface layer (described by $s = 0.8$) of selected samples. The parameter s, commonly used in this context, is defined by the spacing between the layer under inspection and the sheet center layer, counting positive from the center layer, divided by the half thickness, *i.e.*, $s = 0$ indicates the center layer while $s = 0.8$ indicates the subsurface layer. For the measurements, two 14 × 24 mm^2 samples were cut, ground close to the investigated layer, and finally electropolished. The Mo K_α radiation was used in the XRD, and four incomplete pole figures were measured in the back reflection mode. Pole figures (110), (200), (211), and (310) were used for ferritic (α'-martensite) phase and (111), (200), (220), and (311) for the austenite. The orientation distribution functions (ODFs) were calculated using a series expansion method ($l_{max} = 22$) from the pole figure data and plotted in contour lines in the Euler space (Bunge's notation).

III. RESULTS AND DISCUSSION

A. *Martensite Formation during Cold Rolling*

It was demonstrated elsewhere[16] that the Olson–Cohen one-dimensional nucleation-controlled model[24] could be reasonably used in estimating the kinetics of strain-induced martensite formation during rolling. The martensite fraction f is

$$f = 1 - \exp\{-\beta[1 - \exp(-\alpha\varepsilon)]^n\} \quad [1]$$

where ε is the true strain, α and β are parameters dependent on temperature and the stacking fault energy of the steel, and n is the fixed exponent equal to 4.5. In the case of the pass reduction about 5 pct, the values $\alpha = 2.2$ and $\beta = 4.4$ gave a good fit for 301LN. Cold rolling of about 55 pct was found to be adequate to realize nearly 100 pct martensite in 301LN steel. It was also found that a high pass reduction (~15 pct) resulted in lower martensite fractions for the same degree of reduction, obviously as a result of intense adiabatic heating. For less metastable grade 301 the maximum martensite fraction obtained was about 60 pct, and for the experimental heats 100 pct martensite was obtained already at 40 pct reduction (*cf.* M_{d30} temperatures in Table I).

B. *α'-γ Reversion Kinetics*

Upon annealing, the martensite formed during cold rolling reverts back to the austenite. The reversion phenomenon can occur either by martensitic shear or diffusional transformation and this has been well described in the literature for a number of Cr-Ni or austenitic stainless steels.[8,9,13] A brief review of the typical transformation kinetics as a function of annealing temperature for isochronal treatment (1 to 10 seconds holding) for 301LN steel cold rolled to different reductions (45, 60, and 75 pct) is reproduced in Figure 1.[16,17] The reversion temperature range has been found to be about 100 °C in a time-controlled process suggesting diffusional reversion. However, the process was quite fast, so that even in 1 second holding, the 45 pct cold-rolled specimen showed nearly complete transformation beyond 750 °C. However, at longer holding times of 10 seconds, there was practically insignificant difference in reversion kinetics. The total austenite fraction (X) at annealing time t (in seconds) can be fairly accurately predicted by the following Avrami-type equations (as shown by dashed lines in Figure 1).

$$X = X_R + [1 - \exp\{-0.693 \times (t/t_{50})^{n'}\}] \times (1 - X_R) \quad [2]$$

$$t_{50} = \mathrm{t} \times \exp\,[Q/R\{1/(T + 273) - 1/(T_X + 273)\}] \quad [3]$$

where X_R is the untransformed austenite fraction, t_{50} is the time for 50 pct reversion transformation, n' is an exponent for Avrami-type fit, T is the annealing temperature (in °C), T_X (in °C) is the temperature for 50 pct reversion from martensite to austenite in time t (in seconds) dependant on cold-rolling (CR) reduction, Q is the activation energy of transformation (in J/mol K), and R is the universal gas constant. While X_R can be modeled as using the Olson and Cohen equation (Eq. [1]), Q has been estimated to be ~400 kJ/mol K, slightly varying with cold-rolling reduction, decreasing with increasing strain. Carbide (in 301 steel) or nitride (in 301LN steel) precipitation at higher temperatures (about 800 °C) can lead to depletion of C or N in the reverted austenite, resulting in an increase in M_s temperature above RT, and consequently, some reverted austenite may again transform back to martensite.[19] This was further confirmed by magnetic measurements (SQUID) for 301LN and 301 steels and the gross austenite content was actually found to decrease at higher temperatures. Some differences exist in austenite measurements as using SQUID and XRD possibly due to texturing effects, but XRD measurements were still found to be reasonable. It was seen that for both 301LN and 301 steels, within these short holding times (1 to 10 seconds), the reversion seems to start around 650 °C

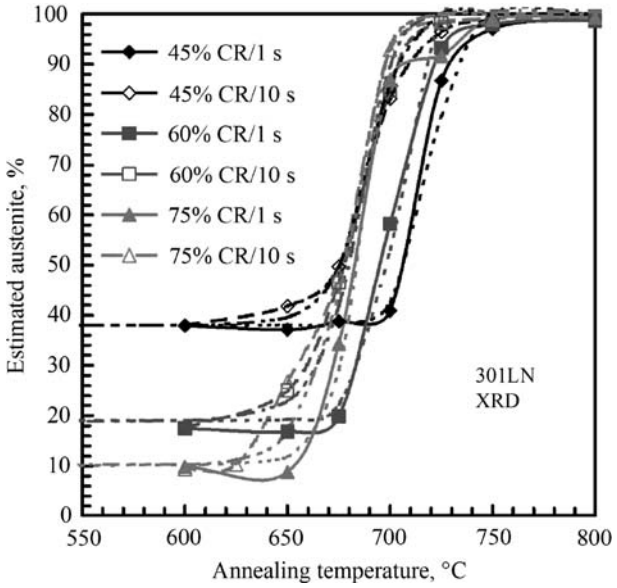

Fig. 1—Reversion of martensite to austenite in 301LN steel on annealing at different temperatures (1 and 10 s) showing the influence of cold-rolling reduction on reversion kinetics.

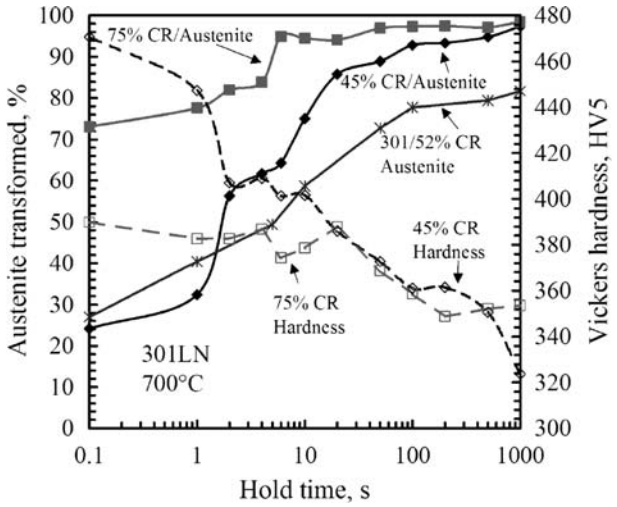

Fig. 2—Effect of cold-rolling reduction on the martensite to austenite reversion kinetics in 301LN as estimated by magnetic and hardness measurements. Transformation data obtained on 301 (52 pct CR) also included for comparison.

and be completed in 301LN steel at 750 °C (Figure 1) and in 301 steel at 800 °C.

Figure 2 presents the reversion kinetics for 301LN upon annealing at 700 °C for two different rolling reductions, 45 and 75 pct CR, as measured by a Ferritescope. It is seen that the transformation rate is dependent on the annealing time and also strongly on the degree of prior cold-rolling reduction. The hardness data are also plotted in the figure; hardness concomitantly decreasing with the increase in austenite fraction as a function of time. It is seen that the reversion process is quite fast at 75 pct CR, so that even without any holding at 700 °C (marked 0.1 seconds), there is extensive reversion (austenite fraction above 70 pct) and it gets nearly completed in about 6 seconds. However, at 45 pct CR, the kinetics are relatively slow so that there was still about 10 pct martensite in the microstructure after about 100 seconds. For comparison, the transformation data for the 301 steel, cold rolled to 52 pct reduction, are also included, showing relatively slower transformation kinetics (austenite fraction ~80 pct in 1000 seconds). For comparison, the XRD measurements showed somewhat higher fractions of austenite than that measured by Ferritescope due to the limitations imposed by either technique.

C. *Microstructures of Reversion-Annealed Stainless Steels*

Figure 3 displays typical optical microstructures obtained for 301LN steel following the reversion annealing in the range 700 °C to 900 °C. There is a wide variation in the microstructures related to the reversion kinetics, which in turn is related to the cold-rolling reduction. It has been illustrated in the literature that the α'-γ reversion by martensitic shear essentially depends on the chemical driving force (*i.e.*, the chemical composition) and is independent of the amount of cold-rolling reduction.[8] Hence, it was further confirmed that in 301LN, the transformation was essentially diffusion controlled, as also supported by the XRD results (Figure 1). The resolution of OM was not sufficient to reveal the finest details, but the formation of fine austenite grains can be seen at 750 °C to 900 °C. The large white grains present in some microstructures (Figures 3(a) and (b), for example) are the retained austenite with the grain sizes up to about 50 μm, deformed during cold rolling. These grains may recrystallize in the course of annealing during longer holding times (Figures 3(d) and (e)). Examples of SEM-EBSD analysis of ultrafine reverted austenite and martensite in 301LN steel (60 to 63 pct CR) following annealing at 800 °C/1 s are reported elsewhere.[16,17] The TEM observations for 301LN steel (62 pct cold-rolling reduction) revealed formation of nanograined austenite already at 600 °C, and the grain size increased rapidly from ~0.1 to ~0.3 μm as the temperature increased from 600 °C to 800 °C, and from ~0.7 to ~4.2 μm as the annealing time changed from 1 to 100 seconds at 800 °C.[19] In addition, specimens reversion-annealed at 800 °C revealed extensive precipitation even in a short duration of 10 seconds.[19] Figure 4 shows examples of typical TEM micrographs of 301LN steel cold rolled to ~63 pct reduction, annealed at 730 °C (Figures 4(a) through (c)) and 800 °C (Figures 4(d) through (f)) for a short annealing time of 1 second. The lower temperature, reheating at 730 °C gave a mixed microstructure of very fine reverted grains (Figure 4(a)), along with deformed retained austenite (Figure 4(b)) and martensite laths (Figure 4(c)). However, increasing the temperature to 800 °C resulted in a mixture of mostly reverted austenite grains (Figure 4(d)), along with some deformed austenite grains showing dislocation pile-ups (Figure 4(e)) and twinned regions (Figure 4(f)) in some areas.

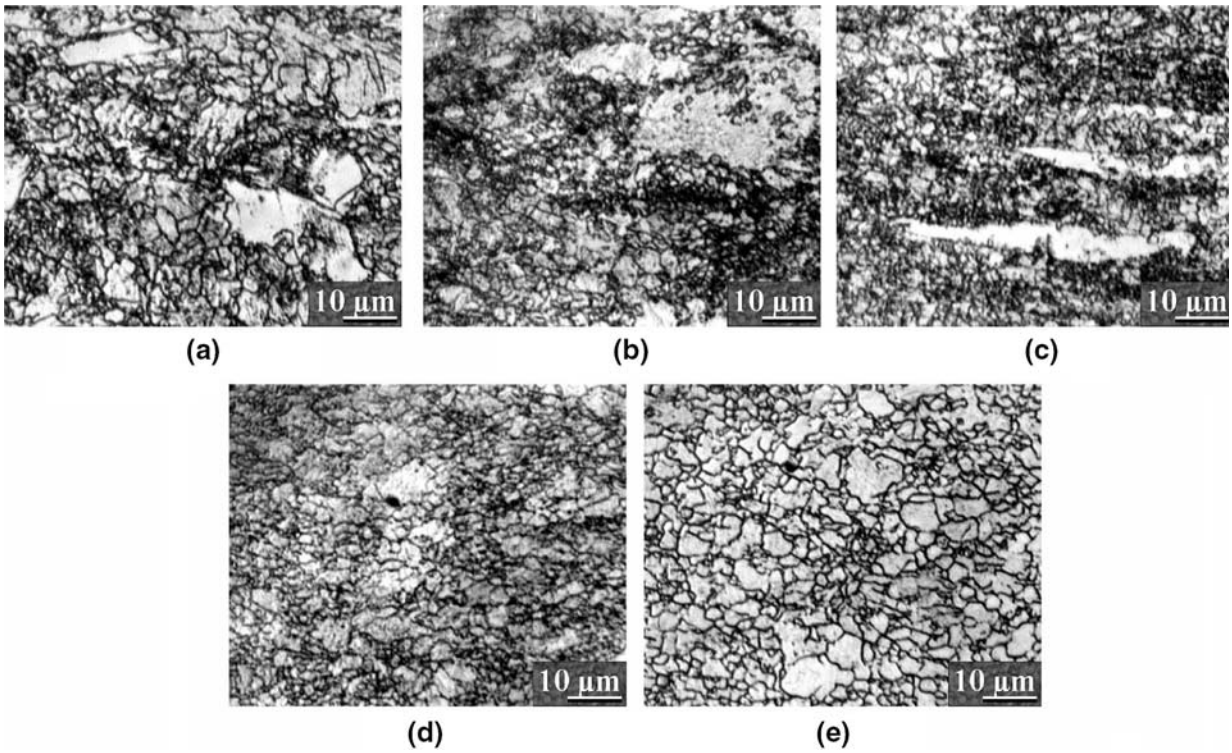

Fig. 3—Typical optical microstructures of 301LN steel showing the influence of cold-rolling reduction and annealing conditions on the reversion characteristics: (*a*) 45 pct CR/750 °C/10 s, (*b*) 62 pct CR/700 °C/1 s, (*c*) 77 pct CR/700 °C/1 s, (*d*) 62 pct CR/800 °C/1 s, and (*e*) 62 pct CR/900 °C/1 s.

Figure 5 shows the typical optical microstructures of 301 steel cold rolled to 52 pct reduction followed by annealing at 800 °C and 900 °C, and held for 10 and 100 seconds. In this case, the transformation appears to be the martensitic shear type, as ultrafine reverted grains typical of diffusional reversion are not seen in the microstructure until about 900 °C, even though the α'-γ reverse transformation was nearly completed in 1 second at 800 °C, as estimated by Ferritescope measurements and XRD as well as later verified by SQUID and electron diffraction analysis.[17,19] The optical microstructure still shows nearly banded, pancaked grains (Figure 5(a)), thus further confirming that the transformation occurred by shear. Since martensitic shear is hardly affected by the cold-rolling reduction and is exclusively determined by the chemical driving force,[8] it was considered appropriate to study only one reduction, *i.e.*, 52 pct CR. On the other hand, static recrystallization can always proceed with time initiating at shear bands of the transformed austenite and also in the retained austenite, due to the stored energy from the cold deformation. Figures 5(b) through (d) show the progress of partial recrystallization resulting in the refinement of the grain size. The resolution of the OM is not adequate to reveal the grain size precisely. In 301 steel (for 52 pct reduction), grains as fine as 70 and 140 nm were seen by TEM following annealing for 100 seconds at 600 °C and 800 °C, respectively.[17,18] Furthermore, some carbide precipitation occurred at 800 °C already within 10 seconds.[25] On the other hand, samples annealed at 1000 °C showed defect-free large austenite grains with high-angle boundaries, occurrence of microtwins, and a significantly reduced number of precipitates.[25]

Figures 6(a) through (c) show the typical microstructures obtained in 17/7N and 17/7C experimental steels deformed to different reductions. The microstructures of all specimens annealed at different temperatures up to 900 °C showed essentially the martensitic shear-type reversion (Figures 6(a) and (b)), irrespective of cold-rolling reduction, *i.e.*, the original pancaked grains are still present, even though the austenite reversion was nearly complete in 1 second by holding at about 800 °C (as revealed by XRD). Holding up to about 10 seconds at 900 °C did not show any significant change in the microstructure for these experimental steels, suggesting slow recrystallization kinetics at 900 °C. However, a slight increase in temperature to 925 °C led to fast recrystallization even in 1 second (Figure 6(c)) and nearly complete recrystallization in 10 seconds. As expected, the kinetics of recrystallization was found to be dependent on the amount of stored energy, *i.e.*, cold reduction.

D. *Reversion Mechanisms*

The temperature dependence of the free energy change between α and γ for the 15.6Cr-9.8Ni and 17.6Cr-8.8Ni metastable austenitic stainless steels has earlier calculated from a regular solution model by Tomimura *et al.*[8] These steels were prepared by induction melting of electrolytic iron, nickel, and metallic chromium chips.

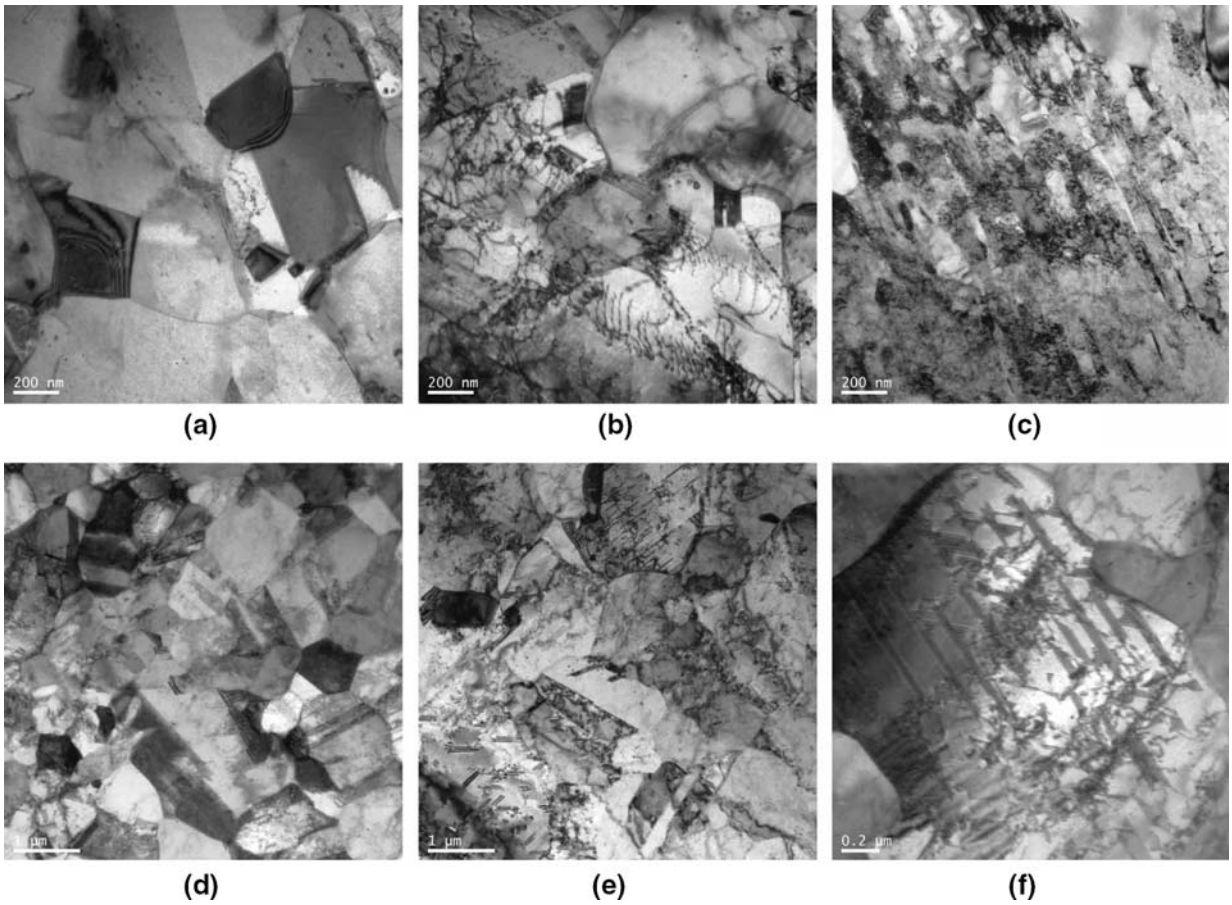

Fig. 4—TEM micrographs showing microstructures of 301LN steel cold rolled to ~62 pct reduction followed by reversion annealing at (*a*) through (*c*) 730 °C/1 s and (*d*) through (*f*) 800 °C/1 s.

Other elements such as C, N (both <0.005 pct, 15.6Cr-9.8Ni) and Si, Mn (both <0.1 pct, 17.6Cr-8.8Ni) were suitably controlled to enable calculation of the temperature dependence of the free energy change between α and γ. Tomimura *et al.*[8,9] have earlier explained that an increase in Ni/Cr ratio caused an increase in the Gibbs free energy change between bcc and fcc structures ($\Delta G^{\alpha\rightarrow\gamma}$ in J/mol) leading to lowering of the shear reversion temperature. The critical driving force for complete martensitic shear reversion was estimated to be about –500 J/mol. The following equation was derived using the thermodynamic data reported by Kaufman *et al.*[26] for the ternary Fe-Cr-Ni system

$$\begin{aligned}\Delta G^{\alpha\rightarrow\gamma}(\mathrm{J/mol}) &= 10^{-2}\Delta G_{\mathrm{Fe}}^{\alpha\rightarrow\gamma}(100-\mathrm{Cr}-\mathrm{Ni}) - 97.5\mathrm{Cr} + 2.02\mathrm{Cr}^2 \\ &\quad - 108.8\mathrm{Ni} + 0.52\mathrm{Ni}^2 - 0.05\mathrm{CrNi} \\ &\quad + 10^{-3}T\left(73.3\mathrm{Cr} - 0.67\mathrm{Cr}^2 + 50.2\mathrm{Ni} - 0.84\mathrm{Ni}^2 \right. \\ &\quad \left. - 1.51\mathrm{CrNi}\right) \end{aligned} \quad [4]$$

where $\Delta G_{\mathrm{Fe}}^{\alpha\rightarrow\gamma}$ is the free energy difference in pure iron, T is temperature in Kelvin, and the symbols of Ni and Cr represent the chemical composition of each element (mass pct). For the 16Cr-10Ni steel, the lowest temperature where deformation-induced martensite could completely revert to austenite martensitically was estimated to be ~650 °C and $\Delta G^{\alpha\rightarrow\gamma}$ at that temperature ≈ –500 J/mol. As using Eq. [4], it can be easily demonstrated that the $\Delta G^{\alpha\rightarrow\gamma}$ is well above –500 J/mol for all the steels, except 16/10. Hence, in principle, martensitic shear reversion should neither take place in 301 or 301LN steels, nor in 17/7N and 17/7C experimental steels, contrary to the observations.

In this study, the previously described criteria (Eq. [4]) governing the temperature dependence of Gibbs free energy change to determine the reversion mechanism was further extended to include the effects of other alloying elements as well, which have strong influence on the microstructure constitution such as Si, Mn, Mo, C, and N.[17] To account for the effects of these alloying elements, it was considered appropriate to use Ni_{eq} or Cr_{eq} instead of just Ni and Cr, respectively, in Eq. [4] to compute the value of $\Delta G^{\alpha\rightarrow\gamma}$. The following equations were deduced by regression, which could tentatively explain the observed microstructures:

$$\mathrm{Ni}_{eq} = \mathrm{Ni} + 0.6\mathrm{Mn} + 20\mathrm{C} + 4\mathrm{N} - 0.4\mathrm{Si} \quad [5]$$

$$\mathrm{Cr}_{eq} = \mathrm{Cr} + 4.5\mathrm{Mo} \quad [6]$$

For Ni_{eq}, the power of individual elements has been considered much in a similar way as has been done by Takemoto *et al.*,[27] where a regression approach was

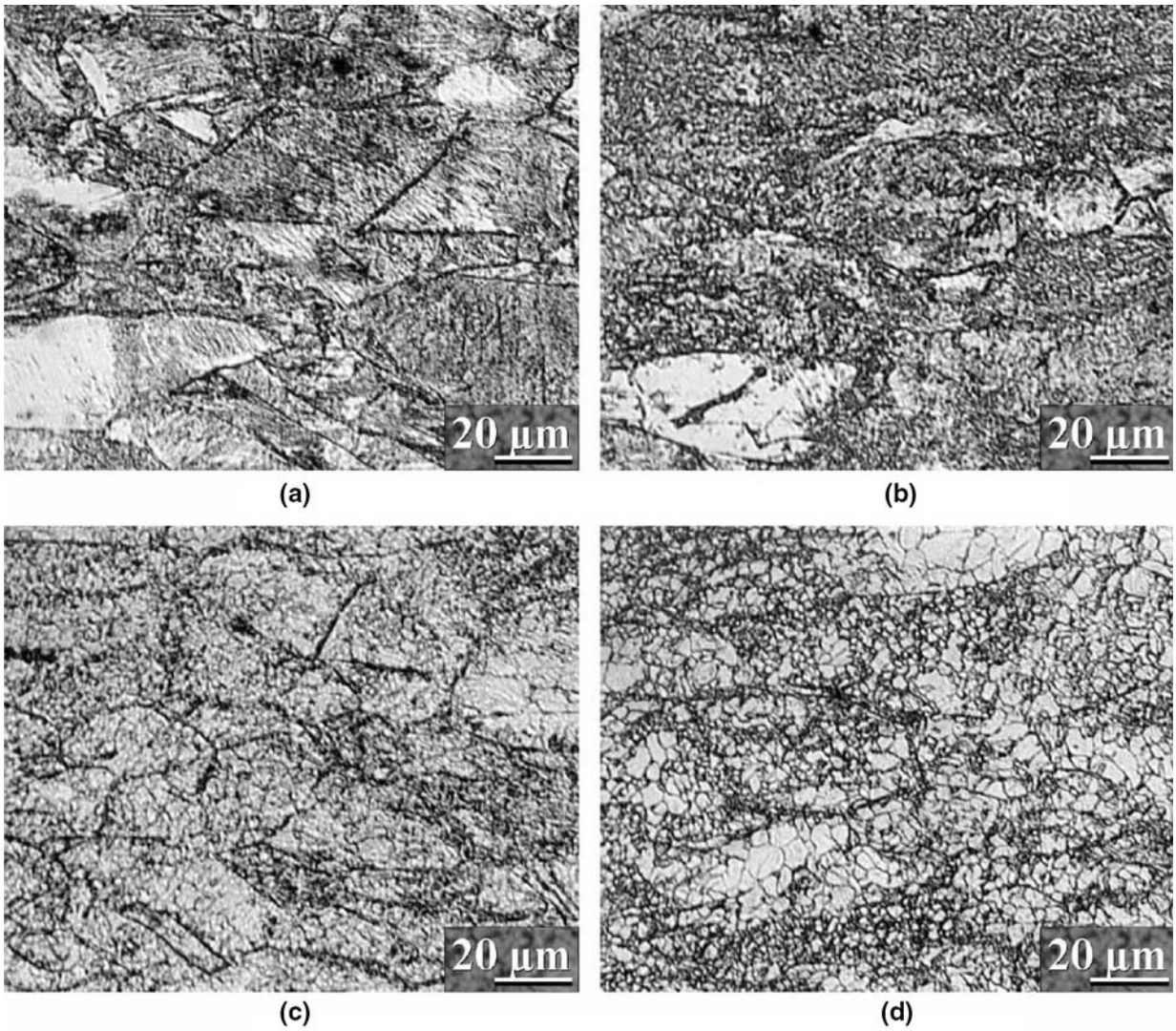

Fig. 5—Optical micrographs showing typical shear reversion from martensite to austenite followed by recrystallization in 301 steel, 52 pct cold rolled and annealed at (*a*) 800 °C/10 s, (*b*) 800 °C/100 s, (*c*) 900 °C/10 s, and (*d*) 900 °C/100 s.

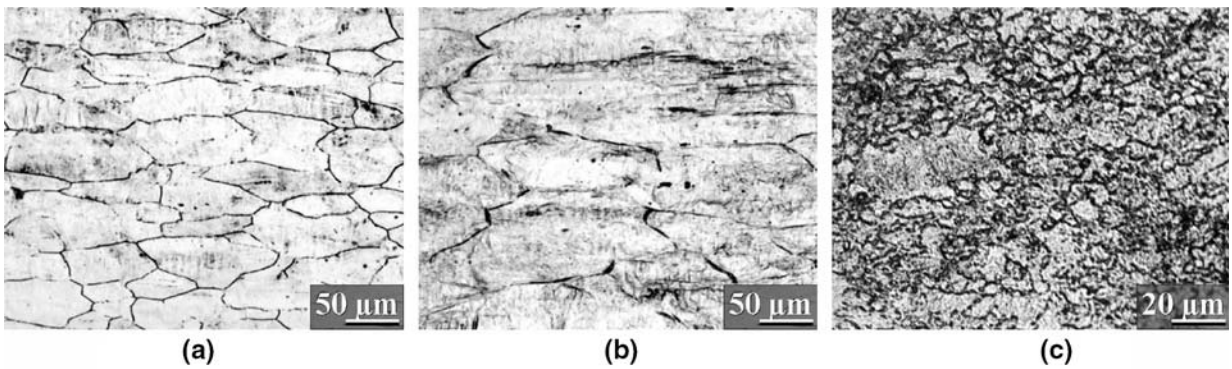

Fig. 6—(*a*) and (*b*) Typical microstructures obtained on experimental steels showing martensitic to austenite reversion by shear, (*c*) followed by ultrafine-grain formation through recrystallization. (a) 17/7N/63 pct CR/900 °C/10 s, (b) 17/7C/67 pct CR/900 °C/10 s, and (c) 17/7N/63 pct CR/925 °C/1 s.

adopted to describe the austenite stability and the effect of alloying elements on strain-induced martensite formation in Fe-Cr-Ni steels. Since Mo is a strong ferrite and carbide former and is known to increase the minimum temperature at which the martensite shear reversion may occur,[28] a higher power has been chosen

for Mo as compared to Cr in computing the Cr_{eq} (Eq. [6]). Figure 7 shows the relation derived between the Gibbs free energy change from martensite to austenite in the steels studied here based on the computation of Ni_{eq} and Cr_{eq} (Eqs. [5] and [6], respectively) in Eq. [4], in lieu of Ni and Cr, respectively. Thus, it was possible to predict that in 301LN the reversion is diffusion controlled, but in 301 steel the shear reversion can occur above the estimated temperature of 670 °C. Likewise, for experimental steels shear reversion can be predicted based on the annealing temperature. Also, it should be noted that since the alloys are not truly Cr-Ni steels, but contain other alloying elements, it is possible that actual $\Delta G^{\alpha\rightarrow\gamma}$ is somewhat different for different alloy systems. Second, the heating rate used in these experiments has been 200 °C/s and still higher heating rates may be necessary in order to induce martensitic shear reversion in 301LN steel.

In essence, new thermodynamic models such as THERMOCALC* might provide more accurate computation of free energy change including possible interaction terms, but the idea in this study was to understand whether Eq. [4][8] could be simply extended to explain the reasons behind the mechanism of reversion by a simple linear regression approach. The alloying elements (C, N, Mo, Si, and Mn) were categorized into ferrite or austenite formers/stabilizers based on the ability of the elements to promote the formation of a certain phase or to stabilize it.[29] This exercise enabled the rationalization of the effects of individual alloying elements by simply replacing the Ni and Cr contents with Ni_{eq} and Cr_{eq} terms in Eq. [4], respectively. Presently, no special efforts were directed to use the THERMOCALC software, which still requires a thorough understanding of the complex mechanisms operating during α and γ reversion in addition to the numerous interaction terms, which might not be accessible.

*Thermocalc is a trademark of Thermo-Calc Software, Stockholm, Sweden.

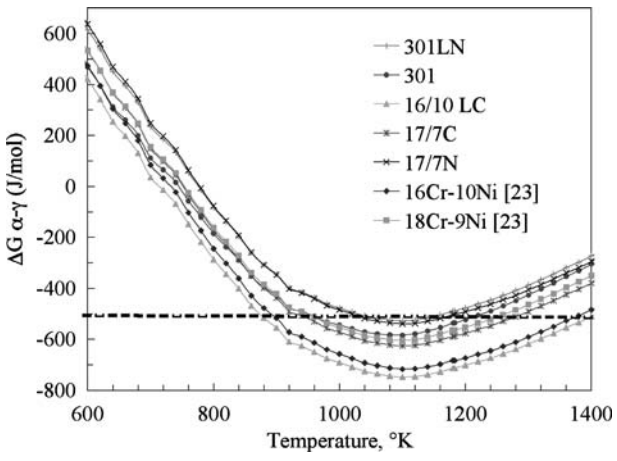

Fig. 7—Relation between temperature and Gibbs free energy changes from martensite to austenite in commercial 301/301LN grades and the experimental steels. Plots for Cr-Ni steels used in Ref. 28 have also been recalculated based on Ni_{eq} and Cr_{eq} and included in the figure.

The diffusional α'-γ reversion, as noticed in 301LN, has been known to occur primarily by nucleation and growth of fine austenite grains at martensite lath boundaries.[9,11] However, a second type of austenite nucleation where reverted intralath γ layers form as thin plates traversing the martensitic laths has also been observed in some specimens, the details of which are described elsewhere.[30] In a parallel study, Rajasekhara *et al.*[31] have recently modeled the kinetics of grain growth in a 63 pct cold-rolled 301LN steel reversion annealed at 800 °C, 900 °C, and 1000 °C for periods of time ranging from 1 to 100 seconds. While the activation energy of grain growth has been found to be similar to those of conventional stainless steels, it was reported that an extremely rapid grain growth occurred during the initial periods of annealing due to the high curvature of grain boundaries and consequently large driving forces for grain growth.[31]

E. *Mechanical Properties*

Tensile properties and hardness as a function of strain-induced martensite formation have been presented in previous articles.[16,17,20] Hence, only a brief review of the mechanical properties with illustrations is given in this section. As an example, the engineering stress-strain curves for both 301LN and 301 steels as annealed at 700 °C to 900 °C for 10 seconds are shown in Figure 8. For sake of comparison, also included in the figure are the stress-strain curves obtained on the three experimental steels annealed at 800 °C. It is obvious that various combinations of yield strength, tensile strength, and elongation are possible to achieve. Some results of numerous tensile tests are collected in

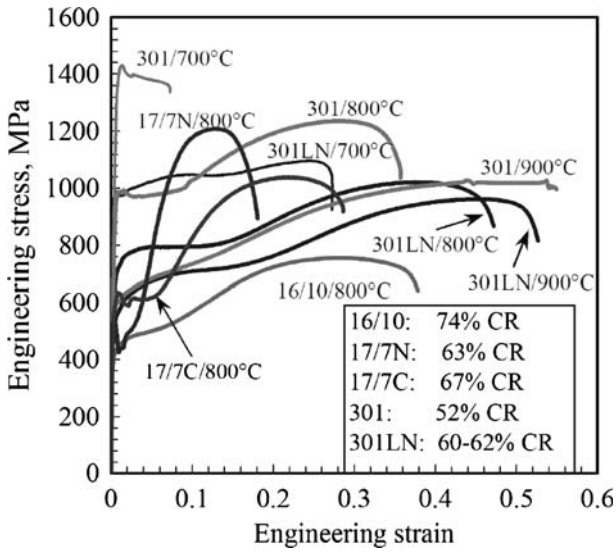

Fig. 8—Typical engineering stress-strain curves for the 301LN and 301 steels reversion annealed at 700 °C, 800 °C, and 900 °C for 10 s. Stress-strain curves obtained on the experimental steels annealed at 800 °C are also plotted for comparison.

Table II. Typical Mechanical Properties after Reversion Annealing and the Martensite Fraction after Tensile Straining

Steel Grade	Annealing Temperature (°C)	Hold Time (s)	$R_{p0.2}$ (MPa)	R_m (MPa)	Ag (Pct)	A20 (Pct)	Martensite after Tension (Pct)
301	25	—	1659	1973	1.2	2	77
(52 pct CR)	700	1	1519	1614	1.2	5	74
	700	10	1303	1418	2	7	98
	800	1	1070	1290	28	28	57
	900	1	584	1032	44	55	48
	900	10	559	1051	59	61	56
301LN	700	1	1223	1342	1.2	8	70
(45 pct CR)	700	10	1062	1209	2	25	58
	725	1	904	1111	24	32	—
	725	10	811	1079	38	45	—
	750	1	783	1067	32	40	73
	750	10	758	1040	35	43	75
	800	1	722	1027	36	45	75
	800	10	624	980	40	49	78
301LN	25	—	1578	1762	1.3	1	—
(60 pct CR)	650	100	1265	1374	1.2	7	43
	650	1000	1090	1219	1.2	15	46
	700	10	918	1119	30	36	76
	700	100	901	1106	31	37	77
	750	0	784	1084	31	38	73
	800	1	711	995	37	50	87
	900	1	595	929	44	55	87
301LN	25	—	1731	1919	1.1	2	—
(76 pct CR)	500	10	2159	2195	0.5	0.7	—
	600	10	1790	1833	0.5	1	94
	700	10	1004	1106	32	38	85
	750	0	836	1112	34	39	70
	800	0	794	1087	35	43	67
	800	1	768	1060	34	43	94
	850	0	722	1048	38	44	62
	900	10	662	1015	41	48	—
16/10	25	—	1044	1137	0.8	2	—
(74 pct CR)	600	10	483	757	23	30	99
	700	10	467	739	28	38	82
	800	10	412	757	28	38	82
	850	10	341	727	30	38	—
	900	10	246	645	35	44	100
17/7N	25	—	1725	1963	0.7	0.8	—
(63 pct CR)	900	10	461	1078	18	19	71
	925	1	476	1134	29	30	75
	950	1	454	1138	31	35	77
17/7C	25	—	1570	1614	0.3	0.3	—
(67 pct CR)	600	10	1506	1532	0.4	0.4	100
	700	10	696	1067	17	23	100
	900	10	531	964	29	32.4	80
	925	1	552	974	27	33.5	85

Table II, along with martensite fractions before and after tensile tests in some cases.

Referring to Table II, the strength of the cold-rolled 301LN steel (and also 301 steel) was very high, reaching the level of 1600 to 1800 MPa at high cold-rolling reductions, but the elongation was only 1 to 3 pct. However, upon the reversion process the strength decreased and the ductility increased sharply beyond the annealing temperature of 600 °C. The cold-rolling reduction does not seem to have a significant effect on the mechanical properties, for even at 45 pct reduction the mechanical properties follow the same trend. An increase in the holding time shifts the drop in strength (and corresponding increase in elongation) only marginally to lower temperatures. Depending on the annealing temperature (700 °C to 900 °C), yield strength ranged from about 1000 to 600 MPa, while the elongation varied from 27 to 52 pct (Table II). These combinations are distinctly better than those obtained for temper-rolled grades,[16] *e.g.*, for C850, typically $R_{p0.2} \approx 650$ MPa and $A \approx 30$ pct.[6]

The shapes of the stress-strain curves clearly reveal the inflexion generally beyond about 10 to 15 pct strain (increasing with annealing temperature or holding time) as an indication of the strain-induced martensitic transformation of the reverted austenite. The new martensite should have a very fine grain size as it was formed from an ultrafine austenite grain structure.

Figure 9 shows a typical example of the progress of the martensitic transformation during tensile deformation for two different grain sizes (<1 μm for fully reverted austenite at 800 °C/1 s and 20 μm polygonal austenite at 1000 °C/10 s), as measured by the Ferritescope (Table - II). It can be seen that martensite formation is enhanced by the ultrafine grain size, as can also be concluded from the shape of the stress-strain curves in Figure 8, the inflexion at about 0.15 and 0.2 strains after annealing at 800 °C and 900 °C, respectively.

In unstable or metastable steels plasticity may be accompanied by phase transformation, *e.g.*, ε or α' martensite, while in more stable grades twinning may contribute. However, it has been reported that both twinning and strain-induced phase transformation are impeded by grain size reduction, due to a complex dependence on the work hardening rate that results in an increased rate of dislocation storage owing to strain incompatibility at grain boundaries.[32,33] Sinclair *et al.*[34] did report a strong grain size dependence of the dislocation storage as well as the grain size dependence of twinning in a stable austenitic stainless steel grade EN 1.4828 (AISI 309). The density of twins increased significantly at higher strains in the coarse grained material, with all grains being significantly twinned. However, in the fine-grained material twins were observed only at higher strains and only in a fraction of the grains.

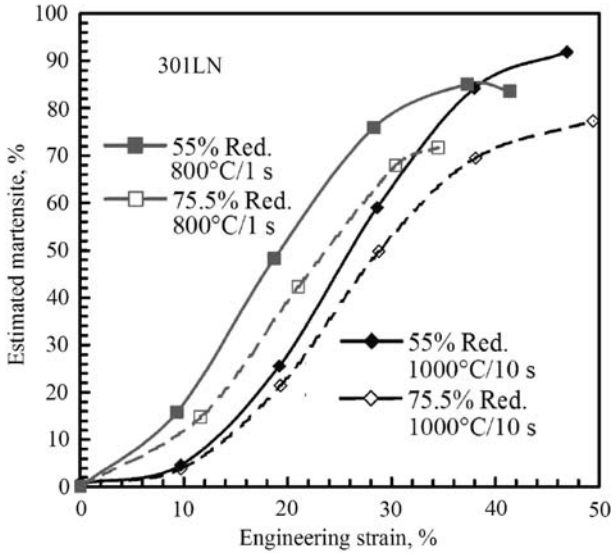

Fig. 9—Progress of martensite formation during RT-tensile straining of the cold-rolled and annealed 301LN steel showing effects of grain size and cold-rolling reduction.

In contrast to the previous observations, in this study on the progress of martensite transformation during tensile straining of the cold-rolled and reversion-annealed 301LN stainless steel (Figure 9), it was found that the kinetics of transformation with straining was faster for an ultrafine grain structure. This means that no such impediment to strain-induced martensite transformation is taking place as a result of reduction in grain size. The plastic deformation should be essentially through dislocation glide in this steel, as no significant twinning has been observed even in the coarse-grained specimens (20 μm, reversion annealed at 1000 °C/10 s). There is a possibility of enhanced formation of strain-induced carbonitride precipitates during reversion annealing of the cold-rolled steel in the vicinity of about 800 °C, as also reported by Rajasekhara *et al.*[19] for the same steel, even in the instance of short holding times (1 to 10 seconds). This precipitation can deplete the austenite of carbon and nitrogen and thereby significantly reduce the stability of austenite leading to enhanced formation of martensite during tensile straining compared to that observed in the coarse grained

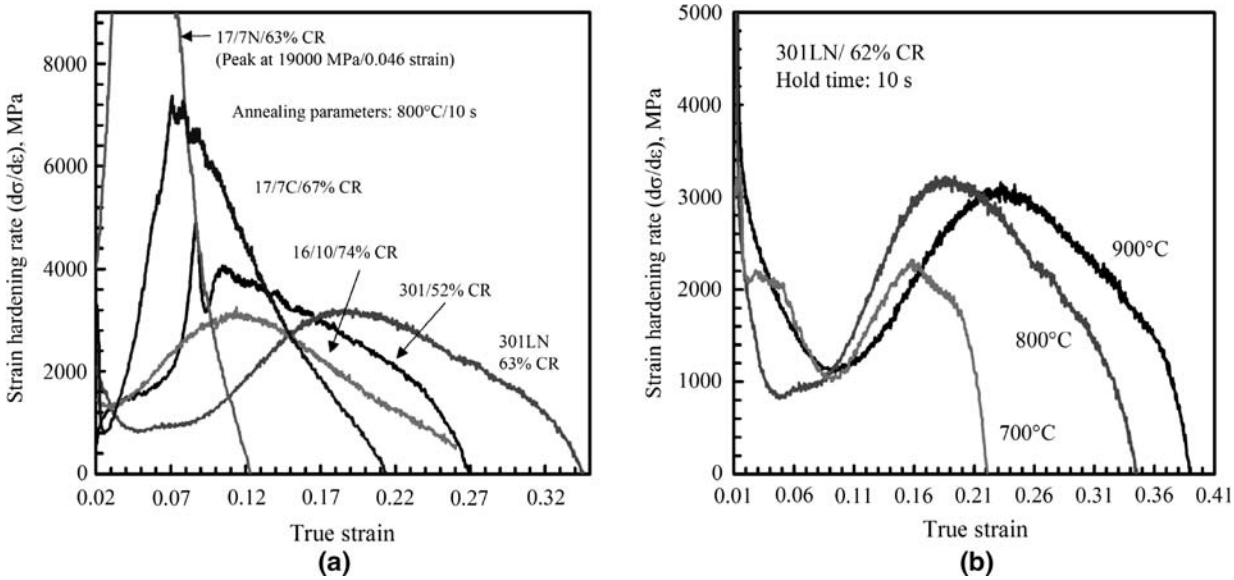

Fig. 10—Typical strain hardening rates ($d\sigma/d\varepsilon$) for the investigated steels (*a*) as reversion annealed at 800 °C for 10 s and (*b*) the effect of reversion temperature in 301LN steel.

specimens annealed at temperatures above the precipitation range. However, this tentative conclusion needs to be further confirmed by TEM analysis.

It is interesting to notice from Figure 8 that the steels 17/7N and 301, for instance, have the same tensile strength (after annealing at 800 °C/10 s), but their ductility is very different. The similar couple is 17/7C and 301LN, having equal tensile strength but very different elongation-to-fracture. It is obvious that the prerequisite for an excellent combination of high strength and ductility is the proper metastability. Too high instability of 17/7N and 17/7C steels (indicated by high M_{d30} temperatures as well, Table I) results in too early formation of martensite and consequently in low ductility. Another remark is that both 301LN and 301 steels seem to possess good combinations of strength-ductility (in fact, somewhat better for 301 than for 301LN in Table II), even though their reversion mechanisms are different, and consequently their microstructures are different ultrafine-grained austenite or highly dislocated coarse-grained austenite, respectively. Hence, it seems that ultrafine grain size is not crucial even

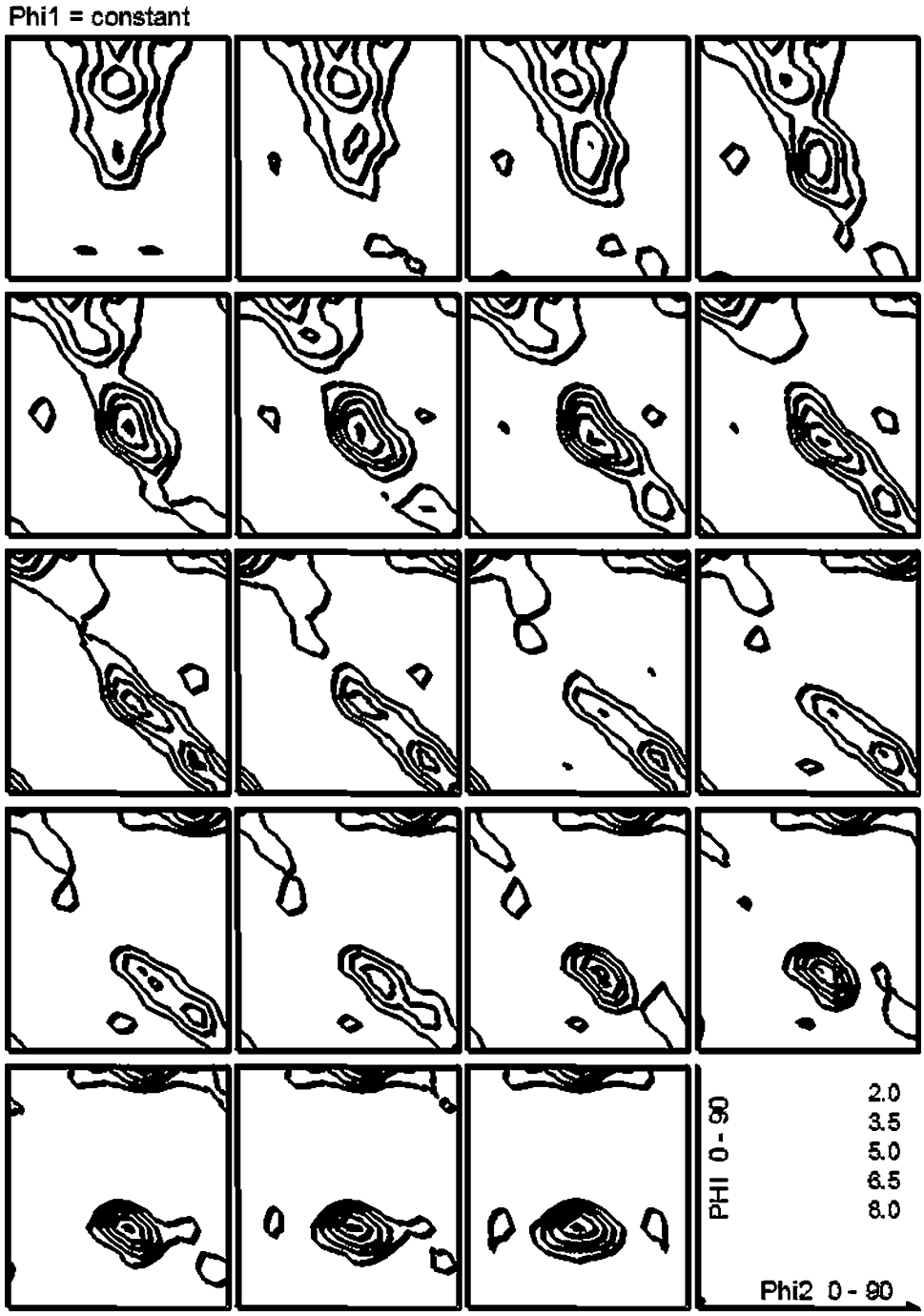

Fig. 11—Cold-rolling texture of the strain-induced α′-martensite in 60 pct cold-rolled 301LN steel (α′-fraction 80 pct).

though its contribution can be quite considerable (about 250 MPa) as predicted by Rajasekhara *et al.*[35] However, this can obviously be compensated by a higher dislocation density.

A plot of strain hardening rate ($d\sigma/d\varepsilon$) against true strain from selected stress-strain curves would further clarify the strain-induced martensite transformation and high uniform elongation. Examples of strain hardening rates for 301LN and 301 steels as well as the experimental steels annealed at 800 °C/10 s, are shown in Figure 10(a). As illustrated in Figure 8, the strain hardening rates are quite high in 17/7N (peak at ~19,000 MPa) and 17/7C (peak at ~9000 MPa) experimental steels and the peak values are attained at very small true strains of 0.045 and 0.075, respectively. In comparison, the hardening rate is somewhat lower in 301 steel (peak at ~4500 MPa) and it peaks at about 0.09 strain, close to 16/10 experimental steel (peak ~3000 MPa at 0.11 strain). All these steels transformed by shear reversion, thus inheriting the original coarse pancaked grains with high dislocation densities. On the other hand, the 301LN steel with ultrafine reverted submicron grains rendered a lower strain hardening rate (~3100 MPa) peaking at about 0.18 strain. As expected, a decrease in annealing temperature to 700 °C resulted in lowering of the strain hardening ability and even faster formation of α' at lower strains (peak rate 2200 MPa at 0.15 strain, Figure 10(b)), obviously as a consequence of the mixed martensite-austenite microstructure at these conditions (Figure 3(b)). However, increasing the annealing temperature to 900 °C, the strain to peak hardening rate increased to ~0.24 strain (Figure 10(b)) without a change in the level of strain hardening rate due to lower rate of α' formation following the coarsening of grain size to ~3 to 4 μm (*cf.* Figure 9). It is noteworthy that despite the higher stability of 301 steel compared to 301LN steel on the basis of the chemical compositions (M_{d30} in Table I), the high dislocation density inherited during shear reversion in 301 steel renders it less stable during subsequent tensile straining and results in high strain hardening rate at lower strains.

F. *Texture Development*

1. *Cold-rolling textures*

After cold rolling, the texture of α' phase in 301LN steel was similar to that in ferritic steels cold rolled at very high reductions, *i.e.*, the texture is dominated by the strong γ-fiber ($\{111\}$ parallel to the rolling plane) and the α-fiber ($\langle 110 \rangle$ parallel to the rolling direction). The texture of martensite was sharp already at 45 pct

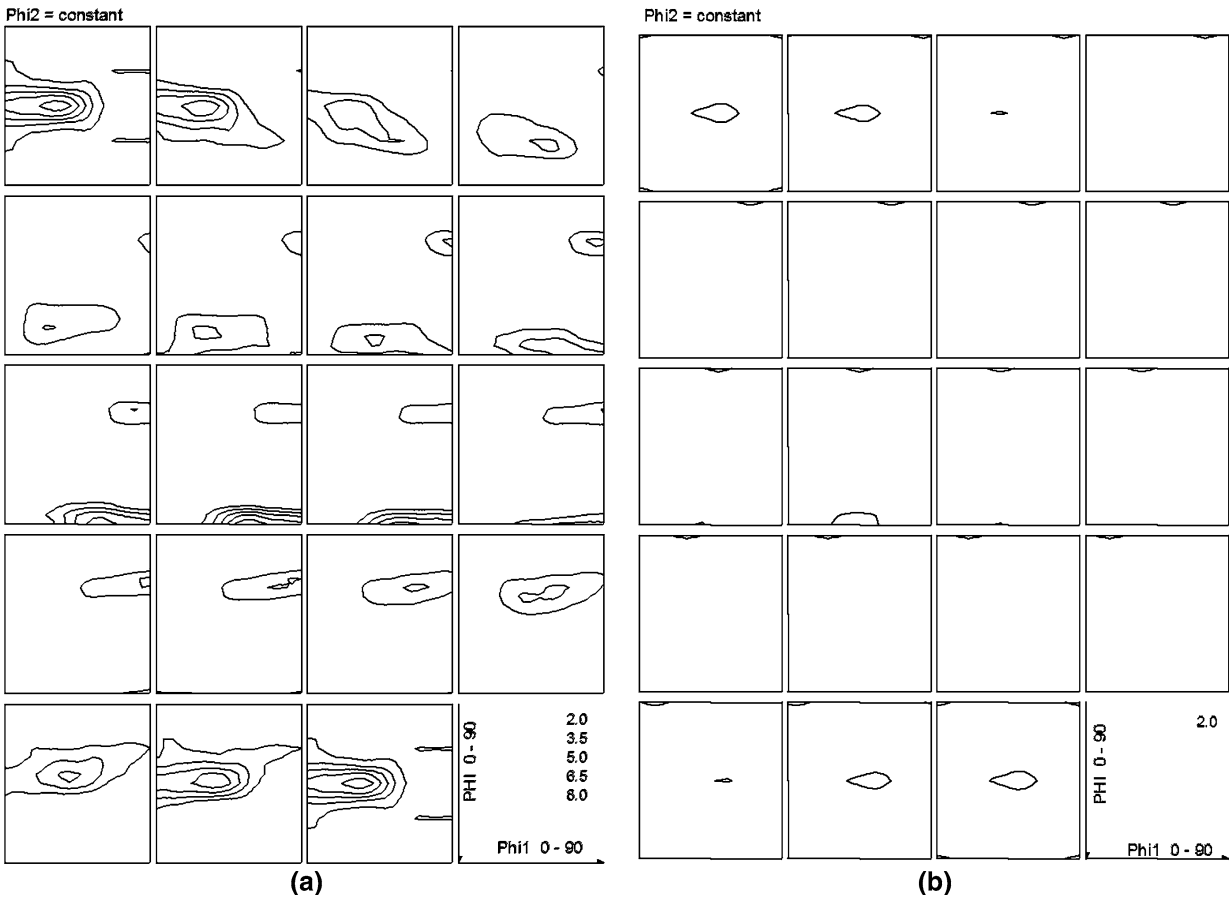

Fig. 12—Textures in 301LN steel in (*a*) 75 pct cold-rolled and reversion-annealed (850 °C/1 s) and (*b*) a commercial cold rolled and annealed condition.

reduction, but it still strengthened at higher reductions. The cold-rolling texture of the 301LN steel at 60 pct rolling reduction containing 80 pct of α′-martensite is shown in Figure 11.

The formation of γ-fiber orientations in the α′-martensite can be explained by the widely accepted Kurdjumov–Sachs orientation relationship.[36] According to that, the close-packed direction ⟨110⟩ of austenite is parallel to that of ⟨111⟩ martensite. Thus, Brass {011}⟨211⟩ and Goss {011}⟨100⟩ orientations of austenite can be regarded as parent orientations of γ-fiber {111}⟨*uvw*⟩ in the strain-induced martensite. Similarly, close-packed plane {111} of the austenite is parallel to {110} of martensite and therefore Copper {112}⟨111⟩ orientation in austenite is at the bottom of α-fiber {*hkl*}⟨110⟩ orientations. In addition, the high intensity of α-fiber in martensite can be explained by deformation. The fraction of the martensite, formed at the early stages of cold rolling, may rotate during further rolling toward the {*hkl*}⟨110⟩ orientations, which are known as stable end orientations of the rolling textures in bcc metals.[37]

2. *Textures of reverted austenite*

Upon reversion annealing, the strong rolling texture of the α′ phase is replaced by the texture of austenite dominated by strong Brass and Goss orientations and minor Copper and S {123}⟨634⟩ orientations. The former martensite γ-fiber orientations adopt their parent orientations Brass and Goss in the austenite. Similarly, Copper and S orientations have their origins in the α-fiber orientations, especially {001}⟨110⟩ of martensite.[38] The martensitic transformation and reversion may strengthen the final texture, but similar texture could also be attained in stable austenite at high cold-rolling reductions. The texture of the reverted fine-grained austenite is very strong compared to the typical texture of commercial cold-rolled and annealed 301LN steels. In Figure 12, the texture of 75 pct cold-rolled and 850 °C/1 s annealed 301LN steel is compared with the texture of a conventionally annealed 301LN steel.

With prolonged annealing, the texture changed during the grain growth in the 301LN steel. The major orientations Brass and Goss weakened and the minor Copper and S orientations disappeared completely. In addition, the formation of an entirely new orientation, {001}⟨100⟩ Cube, was detected, as shown in Figure 13. Regardless of the weakening of the overall texture, it still remained clearly sharper than in conventional 301LN steels.

In the shear-type reversion, which was detected in 301 and experimental steels, a sharp texture with strong Brass and Goss and minor Copper and S orientations appeared immediately after the transformation while the structure consisted of large austenite blocks. With

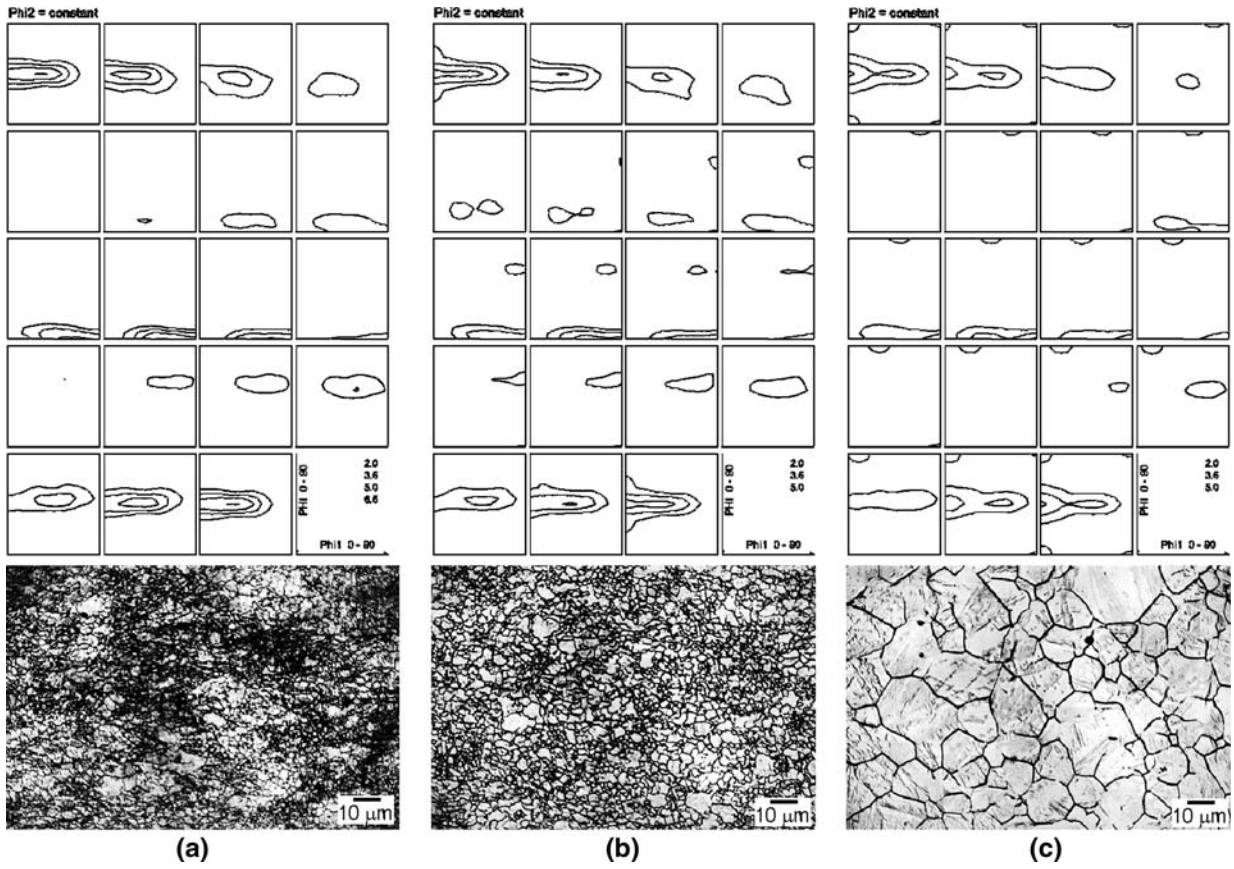

Fig. 13—Texture development during grain growth in 60 pct cold-rolled 301LN steel: (*a*) 800 °C/1 s, (*b*) 900 °C/1 s, and (*c*) 900 °C/1000 s.

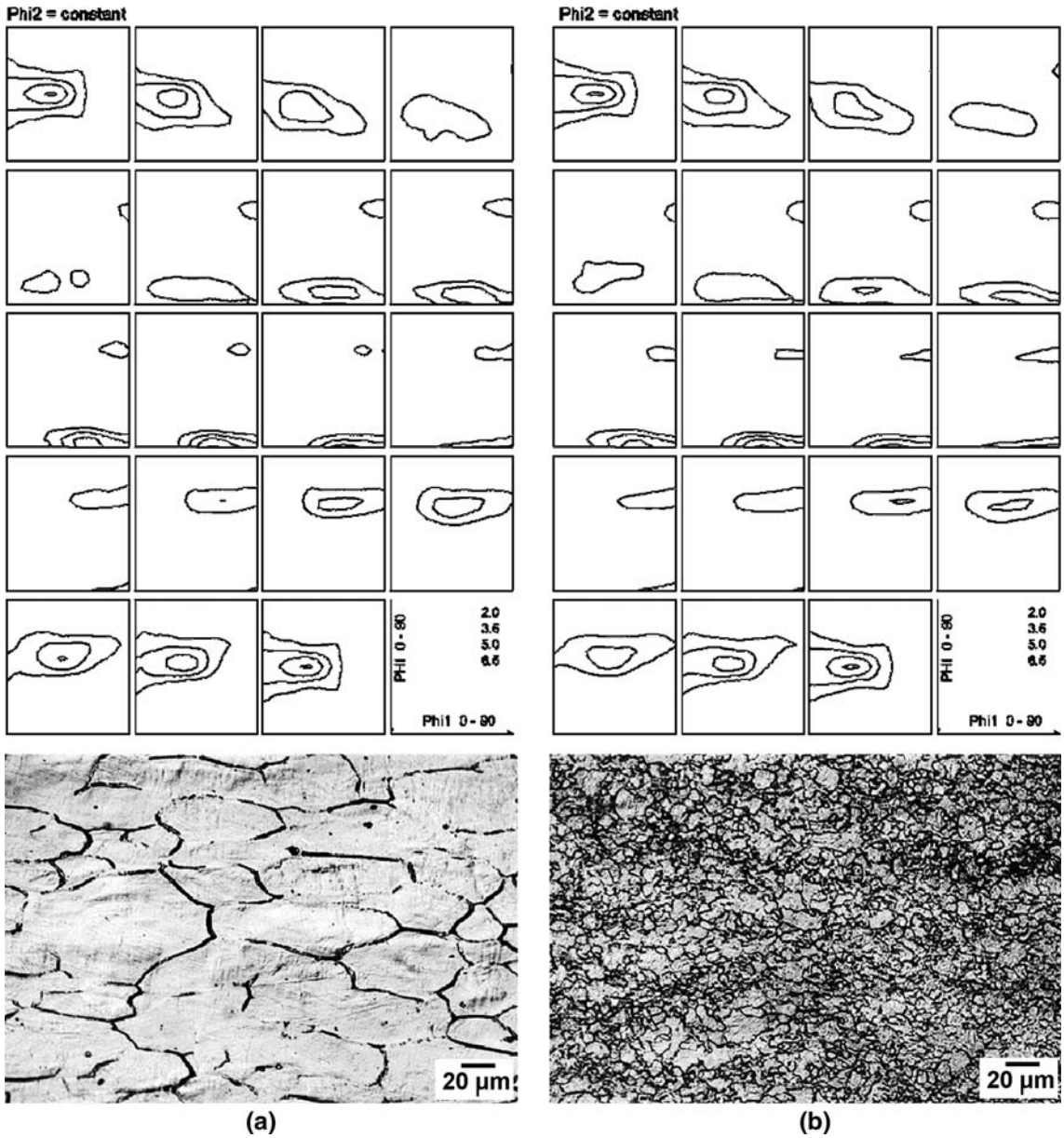

Fig. 14—Textures of 63 pct cold-rolled 17/7N steel. (*a*) Texture of austenite blocks after shear reversion (800 °C/1 s) and (*b*) texture of recovered and recrystallized structure (1000 °C/1 s).

increasing annealing temperature, recovery and recrystallization of the blocks took place but the overall texture remained unchanged (Figure 14). Hence, the reversion mechanism did not affect the texture of the reverted austenite phase. The same main orientations (Brass, Goss, Copper, and S) and equal intensities were found after the reversion annealing irrespective of reversion occurring by the shear or diffusional mechanism. This can be seen by comparing Figures 12(a) and 14, for example.

IV. SUMMARY AND CONCLUSIONS

The novel concept of reverting the strain-induced martensite phase to austenite was successfully applied in two commercial 17Cr-7Ni metastable austenitic stainless steels to achieve excellent combinations of yield/tensile strength and ductility. Low cold-rolling reductions achievable in industrial processing, high heating rate, and very short annealing times were also found acceptable. The following conclusions can be drawn.

While martensite transforms into austenite by the diffusional mechanism in AISI 301LN steel, a martensitic shear-type reversion operates in AISI 301 steel as well as in 17Cr-7Ni-type experimental steels. This means that ultrafine austenite grains are formed directly by the nucleation and growth process from cold-rolled martensite in 301LN, but in the other steels they form by recrystallization from the shear-reverted austenite, thus elucidating the basic difference in the kinetics of the formation of ultrafine grains.

In 301LN steel, even after cold-rolling reductions as low as 45 pct, leaving a considerable amount of cold-deformed austenite in the worked structure, submicron-sized austenite is readily formed in the reversion process. The reversion kinetics were found to be strongly dependent on the prior cold-rolling reduction and annealing conditions, but it is quite fast above 750 °C. On the other hand, the microstructures of 301 and experimental steels showed pancaked banded structure at all temperatures up to about 900 °C regardless of cold-rolling reduction. Fine austenite grains are formed only at higher temperatures or longer annealing times, at 900 °C within 100 seconds, for instance.

However, regardless of the reversion mechanism and the subsequent microstructure, the controlled reversion seems to lead to good mechanical properties both in 301LN and 301 steels. The high performance of 301LN is attributed to the microstructure consisting of ultrafine austenite, deformed austenite, and tempered martensite, and in 301 to shear reverted austenite having adequate dislocation density that leads to gradual strain hardening.

Ultrafine austenite grain size enhances the strain-induced martensite formation in tensile straining. Otherwise, a high dislocation density of austenite (in 301 steel, for example) inherited through shear reversion also increases the instability of austenite and enhances the martensite formation, due to the increased flow stress of these steels during tensile straining. High dislocation density is expected to lead to enhanced strain-induced martensite formation at lower deformation strains, *i.e.*, affecting the stability of the austenite and strain hardening rate.

The criteria governing the temperature dependence of Gibbs free energy change during the martensite-austenite reversion in Cr-Ni steels has been suitably extended in establishing the reversion mechanisms in commercial steels as well as experimental steels by computing Ni_{eq} and Cr_{eq} values instead of using Ni and Cr contents, respectively.

The crystallographic textures of the α'-martensite phase of the cold-rolled 301LN steels were similar to the rolling textures of ferritic steels. Upon reversion annealing the texture of the austenite was dominated by strong Brass and Goss orientations and minor Copper and S orientations, and the reversion mechanism did not affect the texture. The texture of the reverted fine-grained austenite is very strong compared to the typical texture of commercially cold-rolled and annealed 301LN steels.

ACKNOWLEDGMENTS

The financial support from the Finnish Funding Agency for Technology and Innovation (Tekes), Outokumpu Oyj, LaserPlus Oy, and Sanmina-SCI Enclosure Systems Oy in the Tekes-project Nr: 40266/04-Dnr: 2044/31/03 is acknowledged with gratitude.

REFERENCES

1. P.-J. Cunat and T. Pauly: *Proc. 4th Eur. Stainless Steel Science and Market Congr.*, Association Technique De La Siderburgie Francaise, Paris, 2002, pp. 10–18.
2. R. Andersson, E. Schedin, C. Magnusson, J. Ocklund, and A. Persson: *Proc. 4th Eur. Stainless Steel Science and Market Congr.*, Association Technique De La Siderburgie Francaise, Paris, 2002, pp. 57–60.
3. T. Christiansen and M.A.J. Somers: *Metall. Mater. Trans. A*, 2006, vol. 37A, pp. 675–82.
4. *Design Manual for Structural Stainless Steel*, 3rd ed., Euro Inox and The Steel Construction Institute, Luxembourg, 2006, p. 19.
5. A. Kyröläinen: Outokumpu Stainless Oy, Tornio, Finland, process data, 2005.
6. M. Buccioni, L. Alleva, and M. Barteri: *Proc. 5th Eur. Stainless Steel Science and Market Congr.*, J.A. Odriozola and A. Paul, eds., Centro De Investigaciones Cientificas Isla De La Cartuja, Universidad de Sevilla, Seville, Spain, 2005, pp. 31–36.
7. Y. Ma, J.-E. Jin, and Y.-K. Lee: *Scripta Mater.*, 2005, vol. 52, pp. 1311–15.
8. K. Tomimura, S. Takaki, and Y. Tokunaga: *ISIJ Int.*, 1991, vol. 31 (12), pp. 1431–37.
9. K. Tomimura, S. Takaki, S. Tanimoto, and Y. Tokunaga: *ISIJ Int.*, 1991, vol. 31 (7), pp. 721–27.
10. Y. Yagodzinskyy, J. Romu, P. Nenonen, H. Hänninen: *7th Int. Conf. High Nitrogen Steels 2004*, Ostend, Belgium, Steel Grips, GRIPS' Sparkling World of Steel, 2004, vol. 2, Suppl., pp. 103–12.
11. S. Takaki and T. Suzaki: *Proc. Stainless Steel '9 Science and Market–3rd Eur. Congress*, Associazione Italiana di Metallurgia, Chia Laguna Sardinia, Italy, 1999, vol. 2, pp. 49–54.
12. S. Takaki, K. Tomimura, and S. Ueda: *ISIJ Int.*, 1994, vol. 34 (6), pp. 522–27.
13. S. Takaki and Y. Tokunaga: *Proc. 1st European Stainless Steel Conf.*, Florence, Italy, 1993, pp. 2.327–2.332.
14. X.H. Chen, J. Lu, L. Lu, and K. Lu: *Scripta Mater.*, 2005, vol. 52, pp. 1039–44.
15. D.L. Johanssen, A. Kyröläinen, and P.J. Ferreira: *Metall. Mater. Trans. A*, 2006, vol. 37A, pp. 2325–38.
16. M.C. Somani, L.P. Karjalainen, M. Koljonen, P. Aspegren, T. Taulavuori, and A. Kyröläinen: *Proc. 5th Eur. Stainless Steel Science and Market Congr.*, J.A. Odriozola and A. Paul, eds., Centro De Investigaciones Cientificas Isla De La Cartuja, Universidad de Sevilla, Seville, Spain, 2005, pp. 37–42.
17. M. Somani, P. Karjalainen, P. Juntunen, S. Rajasekhara, P. Ferreira, A. Kyröläinen, T. Taulavuori, and P. Aspegren: *Iron and Steel*, vol. 40, pp. 283–89; *Int. Conf. HSLA Steels 2005 and ISUGS 2005*, Sanya, China, 2005.
18. S. Rajasekhara, M.C. Somani, L.P. Karjalainen, A. Kyröläinen, and P.J. Ferreira: *Iron and Steel*, vol. 40, pp. 232–37; *Int. Conf. of HSLA Steels 2005 and ISUGS 2005*, Sanya, China, 2005.
19. S. Rajasekhara, M.C. Somani, M. Koljonen, L.P. Karjalainen, A. Kyröläinen, and P.J. Ferreira: *MRS 2005 Fall Meeting*, Materials Research Society, Boston, MA, 2006, vol. 903E, pp. 40.1–40.6.
20. M.C. Somani, L.P. Karjalainen, A. Kyröläinen, and T. Taulavuori: *Mater. Sci. Forum*, 2007, vols. 539–543, pp. 4875–80.
21. J. Talonen, P. Nenonen, G. Pape, and H. Hänninen: *Metall. Mater. Trans. A*, 2005, vol. 36A, pp. 421–32.
22. K. Nohara, Y. Ono, and N. Ohashi: *J. Iron Steel Inst. Jpn.*, 1977, vol. 63, pp. 212–22.
23. R.L. Miller: *Trans. ASM*, 1968, vol. 61, pp. 592–97.
24. G.B. Olson and M. Cohen: *Metall. Trans. A*, 1975, vol. 6A, pp. 791–95.
25. S. Rajasekhara, P.J. Ferreira, L.P. Karjalainen, and A. Kyröläinen: *Proc. 6th Eur. Stainless Steel Conf. Science and Market*, P. Karjalainen and S. Hertzman, eds., Jernkontoret, Helsinki, Finland, 2008, pp. 505–10.
26. L. Kaufman, E.V. Clougherty, and R.J. Weiss: *Acta Metall.*, 1963, vol. 11, pp. 323–35.
27. T. Takemoto, Y. Murata, and T. Tanaka: *ISIJ Int.*, 1990, vol. 30 (8), pp. 608–14.
28. K. Tomimura, S. Takaki, and Y. Tokunaga: *J. Iron Steel Inst. Jpn.*, 1990, vol. 76 (10), pp. 1728–35.
29. K.-E. Thelning: *Steel and Its Heat Treatment*, Bofors Handbook, Butterworth and Co., London, 1975, pp. 82–126.

30. M.C. Somani, L.P. Karjalainen, R.D.K. Misra, P. Juntunen, and A. Kyröläinen: *Proc. 6th Eur. Stainless Steel Conf. Science and Market*, P. Karjalainen and S. Hertzman, eds., Jernkontoret, Helsinki, Finland, 2008, pp. 519–24.
31. S. Rajasekhara, P.J. Ferreira, L.P. Karjalainen, and A. Kyröläinen: *Proc. 6th Eur. Stainless Steel Conf. Science and Market*, P. Karjalainen and S. Hertzman, eds., Jernkontoret, Helsinki, Finland, 2008, pp. 511–17.
32. S.K. Varma, J. Kalyanam, L.E. Murr, and V. Srinivas: *J. Mater. Sci. Lett.*, 1994, vol. 13, pp. 107–11.
33. M.A. Meyers, O. Vöhringer, and V.A. Lubarda: *Acta Mater.*, 2001, vol. 49, pp. 4025–39.
34. C.W. Sinclair, H. Proudhon, and J.-D. Mithieux: *Mater. Sci. Forum*, 2007, vols. 539–543, pp. 4714–19.
35. S. Rajasekhara, P.J. Ferreira, L.P. Karjalainen, and A. Kyröläinen: *Metall. Mater. Trans. A*, 2007, vol. 38A, pp. 1202–10.
36. G.V. Kurdjumov and G. Sachs: *Z. Phys.*, 1930, vol. 64, pp. 325–43.
37. M. Hölscher, D. Raabe, and K. Lücke: *Steel Res.*, 1991, vol. 62, pp. 567–75.
38. B. Ravi Kumar, A.K. Singh, B. Mahato, P.K. De, N.R. Bandyopadhyay, and D.K. Bhattacharya: *Mater. Sci. Eng. A*, 2006, vol. 429, pp. 205–11.